Journal of Vertebrate Paleontology 25(2):442–450, June 2005

NEW DISCOVERY OF *IRANOTHERIUM MORGANI* (PERISSODACTYLA, RHINOCEROTIDAE) FROM THE LATE MIOCENE OF THE LINXIA BASIN IN GANSU, CHINA, AND ITS SEXUAL DIMORPHISM

TAO DENG
Institute of Vertebrate Paleontology and Paleoanthropology, Chinese Academy of Sciences, P.O. Box 643, Beijing 100044, China, dengtao@ivpp.ac.cn

ABSTRACT—A large-bodied (skull length 775 mm) elasmothere rhinoceros was discovered in the early late Miocene (equivalent to the European Vallesian) Liushu Formation of the Linxia Basin in northwestern China. *Iranotherium morgani*, represented by two skulls and a mandible, is the only known rhinoceros with a rugosity on each zygomatic arch of the male individual. Such a unique cranial feature is otherwise unknown among rhinoceroses. Numerous cranial and dental characteristics indicate that *Iranotherium morgani* is a member of Elasmotheriini, an enigmatic clade of Rhinocerotinae. The large, robust areas on the zygomas of the male *Iranotherium*, for larger masseteric and temporalis musculature, suggest that these rhinoceroses were sexually dimorphic, probably similar to their artiodactyl counterparts in an open grassland fauna.

INTRODUCTION

Elasmotheres are fossil rhinocerotids that are classically considered as being close relatives of living rhinoceroses. Although they were widespread and well diversified throughout the Neogene in Eurasia, most species are still poorly documented. No global revision of the Elasmotheriini was until that of Antoine (2002).

Two nearly-complete skulls and a mandible of the genus *Iranotherium* were discovered from Shanzhuang and Houshan in Guanghe County of the Linxia Basin, Gansu Province, China (Fig. 1). They are similar to the only known species of *Iranotherium*, *I. morgani* (Mecquenem, 1908) from Maragha, Iran. The new fossils are referable to this species. Moreover, the two skulls belong to a male and a female, respectively, and we recognize sexual dimorphism in this species.

The *Hipparion* fauna from the upper Miocene Liushu Formation in the Linxia Basin has three distinct horizons (Deng et al., 2004a). *Iranotherium morgani* was collected from the Shanzhuang and Houshan localities in the middle horizon, also known as the Dashengou fauna (Deng et al., 2004b). The Dashengou fauna has yielded: *Pararhizomys hipparionum*, *Promephitis* sp., *P. hootoni*, *Melodon majori*, *Sinictis* sp., *Ictitherium* sp., *Hyaenictitherium wongii*, *H. hyaenoides*, *Dinocrocuta gigantea*, *Machairodus palanderi*, *Felis* sp., *Tetralophodon exoletus*, *Hipparion chiai*, *H. weihoensis*, *Acerorhinus hezhengensis*, *Chilotherium wimani*, *Iranotherium morgani*, *Chleuastochoerus stehlini*, *Dicrocerus* sp., *Samotherium* sp., *Honanotherium schlosseri*, *Gazella* sp., *Hezhengia bohlini*, and *Miotragocerus* sp.

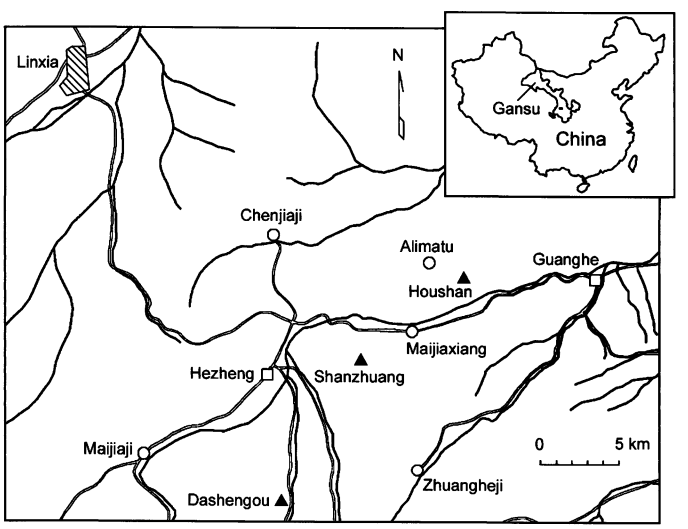

FIGURE 1. Locations of *Iranotherium morgani* from the late Miocene Liushu Formation of the Linxia Basin, Gansu Province, China.

The terminology and taxonomy used in this paper follow those by Heissig (1972, 1999) and Guérin (1980). The measurements are according to Guérin (1980) and are given in mm.

Abbreviations—Institutional: **IVPP**, Institute of Vertebrate Paleontology and Paleoanthropology, Chinese Academy of Sciences, Beijing, China; **HMV**, specimen prefix of Hezheng Paleozoological Museum, Gansu, China; **MNHN**, Muséum National d'Histoire Naturelle, Paris, France. Measurements: **L**, length; **W**, width; **H**, height.

SYSTEMATIC PALEONTOLOGY

Order PERISSODACTYLA Owen, 1848
Family RHINOCEROTIDAE Owen, 1845
Subfamily RHINOCEROTINAE Gill, 1872
Tribe ELASMOTHERIINI Dollo, 1885
Genus *IRANOTHERIUM* Ringström, 1924
IRANOTHERIUM MORGANI (Mecquenem, 1908)
(Figs. 2–7, Tables 1–3)

Lectotype—MNHN 1905-10, skull with left and right P3-M3, and atlas from Maragha, Iran (Mecquenem, 1908:pl. VIII, figs. 1–3, pl. IX, figs. 1–3).

Geographic Distribution—Southwestern Asia (Iran) and East Asia (China).

Stratigraphic Distribution—Late Miocene, Vallesian to Turolian, MN10 to MN12 of Europe, and Baodean of East Asia.

Diagnosis—Large rhinocerotid with huge nasal horn; skull particularly elongate and dorsally concave, with basilar length of 775 mm; parietal crests broadly separate; nasal long and wide, with shallow nasal notch; orbit prominent, its anterior margin situated at level of M3; skull with distinct sexual dimorphism: nasal horn of male much larger than that of female, and strong and rough hemispherical hypertrophy present on posterior part

TABLE 1. Skull measurements (mm) of *Iranotherium morgani*

Measures	HMV 0979	HMV 1098
1 Distance between occipital condyle and premaxillary tip	712	775
2 Distance between nasal tip and occipital condyle	700	745
3 Distance between nasal tip and occipital crest	750	710
4 Distance between nasal tip and notch	145	176
5 Minimal width of braincase	140	123
6 Distance between occipital crest and postorbital process	348	310
7 Distance between occipital crest and supraorbital tubercle	380	355
8 Distance between occipital crest and lacrimal tubercle	453	390
9 Distance between nasal notch and orbit	216	204.5
13 Distance between occipital condyle and M3	330	395
14 Distance between nasal tip and orbit	350	375
15 Width of occipital crest	212.4	190
16 Width between mastoid processes	309	251
17 Minimal width between parietal crests	80	91
18 Width between postorbital processes	244	211
19 Width between supraorbital tubercles	260	253
20 Width between lacrimal tubercles	295	282
21 Maximal width between zygomatic arches	420	340
22 Width of nasal base	140	117
23 Height of occipital face	137	138
25 Heigh of skull in front of P2	173	193
26 Height of skull in front of M1	180	251
27 Height of skull in front of M3	196	259
28 Width of palate in front of P2	67	68
29 Width of palate in front of M1	93	68
30 Width of palate in front of M3	131	77
31 Width of foramen magnum	57	44
32 Width between occipital condyles	183	133

of zygoma of male; posterior part of zygoma uplifted and higher than skull roof; paroccipital process completely fused with post-tympanic process; teeth hypsodont, covered and filled by cement; enamel slightly wrinkled; premolars significantly shortened.

Materials Studied—HMV 0979, complete young male skull (Fig. 2–6, B); HMV 1098, complete adult female skull (Fig. 2–6, A); HMV 1099, adult mandible missing ascending ramus (Fig. 7). All specimens are from the lower part of the upper Miocene Liushu Formation in the Linxia Basin (Gansu, China). HMV 0979 and HMV 1099 were discovered at Houshan village (IVPP Locality: LX0027), and HMV 1098 at Shanzhuang village (LX0008).

DESCRIPTION

Skull—The length from the premaxillary tip to the occipital condyle is 775 mm in the adult. The tooth row is slanted forward and the anterior margin of the orbit is situated at the level of the middle of M3. The nasals are long, with a length of 176 mm from the nasal tip to the bottom of the nasal notch in the adult, and their combined width at the nasal base is 140 mm in the male and 117 mm in the female. The nasal lateral margins are strongly drooped and have a marked lateral process. The nasal tip is pointed and inclined ventrally; it is wide and rough in the male but narrow and smooth in the female. The transverse profile of the nasals is M-shaped. The nasals are fused and have a narrow and deep sagittal groove. The middle nasal horn boss is large and strong in the male, while it is small and weak in the female. The infraorbital foramen is vertically narrow and is located in the middle of the maxillary surface at the level of M1. The nasal notch is shallow and U-shaped and is situated at the level of the P2/P3 boundary. The premaxillae are long and lack upper incisors; they are narrow anteriorly and have a thin edge on the posterior region of their interior walls; their tips are rounded, separate, and slightly uplifted. The nasal-lacrimal suture is long. The facial region of the lacrimal in front of the orbit is flat and smooth, but has a well-developed lacrimal tubercle. The orbit is prominent and has a high position close to the skull roof; its anterior margin is situated at the level of M3. The postorbital

TABLE 2. Mandible measurements (mm) of *Iranotherium morgani*

Measures	HMV 1099
1 Length	~540
2 Distance between symphysis and angular process	455
3 Height of horizontal ramus in front of p3	55
4 Height of horizontal ramus in front of p4	64
5 Height of horizontal ramus in front of m1	70
6 Height of horizontal ramus in front of m2	81
7 Height of horizontal ramus in front of m3	83
8 Height of horizontal ramus posterior to m3	84
9 Distance between horizontal rami in front of m1	56
10 Distance between horizontal rami in front of m3	60.5
11 Length of symphysis	~90
13 Antero-posterior diameter of ascending ramus	150

TABLE 3. Dental measurements (L × W × H, mm) of *Iranotherium morgani*

Upper teeth	HMV 0979	HMV 1098	Lower teeth	HMV 1099
DP1	31 × 26 × 32.5	29 × 28 × 28		
P2	37 × 37 × 30	23 × 37.5 × 30	p2	33 × 22 × 27
P3	44 × 49 × 42	32 × 54 × 29	p3	39 × 34 × 33
P4	46 × 64 × 38	41 × 65.5 × 32	p4	44.5 × 36.5 × 36.5
M1	63 × 71 × 39	43.5 × 76 × 28.5	m1	52.5 × 38 × 42
M2	76.5 × 60.5 × 99	63.5 × 84 × 30	m2	77 × 39.5 × 44.5
M3	62 × 50.5 × 51	79 × 66 × 43	m3	71.5 × 38.5 × 75.5

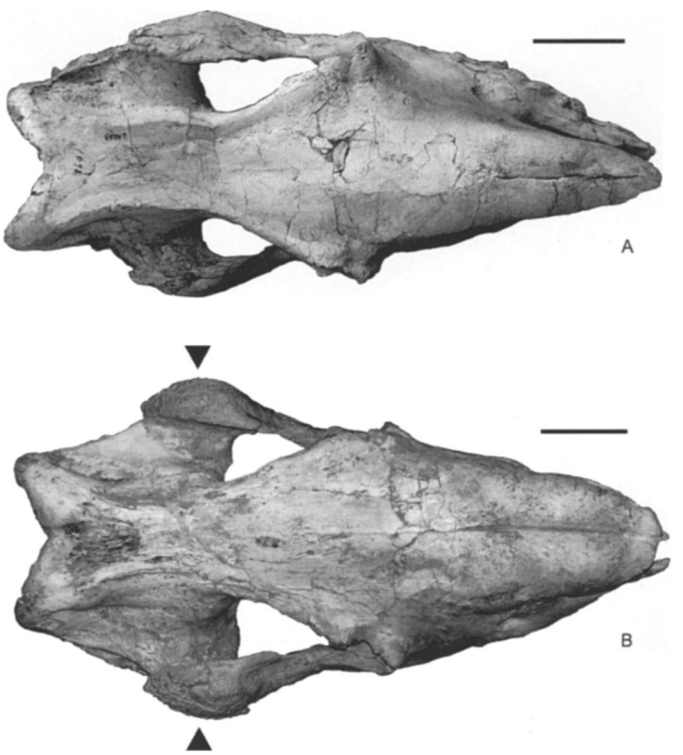

FIGURE 2. Skulls of *Iranotherium morgani*, dorsal view, from the Liushu Formation. **A**, HMV 1098, female, from Shanzhuang; **B**, HMV 0979, male, from Houshan, black arrows indicate rough hemispherical hypertrophies. Scale bars equal 10 cm.

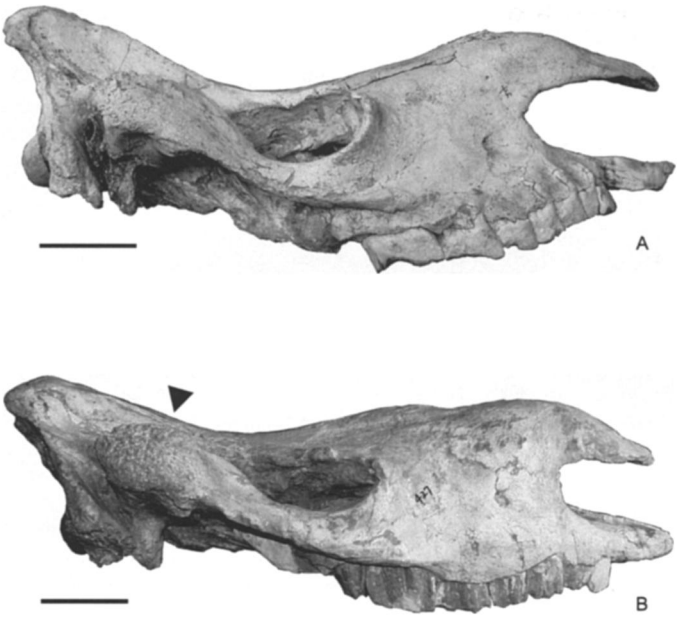

FIGURE 3. Skulls of *Iranotherium morgani*, lateral view. **A**, HMV 1098, female, inverse, from Shanzhuang; **B**, HMV 0979, male, from Houshan, black arrow indicates rough hemispherical hypertrophy. Scale bars equal 10 cm.

process in the frontal is weak or absent. The boundary between the orbit and the sphenoid fuses to form a wide, deep groove. The anterior end of the zygomatic arch is narrow and forms a facial crest, but has no postorbital process. The zygoma is rooted at the level of the anterior region of M3 and has a ventral groove to receive the maxilla. Its mid-section is slender, about 20 mm thick. The posterior region of the zygoma is strongly uplifted so that it is close to or higher than the skull roof. The lower margin of the zygomatic arch is slightly curved. The zygoma also widens posteriorly, more so in the male than in the female, and forms a strong hemispherical hypertrophy with a very rough surface behind the postglenoid process in the male; the hypertrophy is absent in the female. The posterior margin of the zygomatic arch is rounded in the male, but is straight in the female.

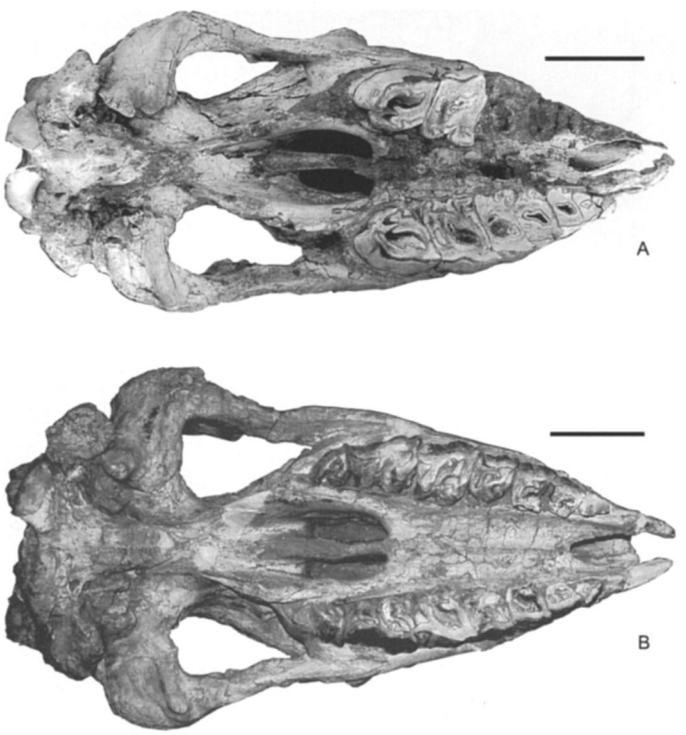

FIGURE 4. Skulls of *Iranotherium morgani*, ventral view. **A**, HMV 1098, female, from Shanzhuang; **B**, HMV 0979, male, from Houshan. Scale bars equal 10 cm.

The dorsal skull profile is strongly concave and forms a deep saddle with an elevated lambdoidal crest. The skull roof is the widest at the level of the lacrimal tubercle, at 282–295 mm. The frontal is convex in its anterior region, but flat in its posterior region, and lacks a horn boss. The braincase is low and wide and has steep orbital walls. The parietal crests are broadly separated by a flat surface at a minimal width of 80–91 mm.

The occipital surface is slanted ventrally and anteriorly. The lambdoidal crest is strong but the nuchal tubercle is weak. The outline of the occipitus is trapezoid. The median crest is weak and the external crest is absent, but the lateral lambdoidal crest is strong. The lambdoidal crest is concave near the mid-line, but more so in the dorsal view than in the posterior view. The lambdoidal crest diverges ventrally and anteriorly. The foramen magnum is onion-shaped and its upper margin is at the same level as the upper border of the occipital condyle. The nuchal ligament depression is a large, deep, inverse triangle. The condyle has flat upper, straight medial, and rounded lower borders. The odontoidal notch between the condyles is broad, with a width of 16.5–23 mm.

The posterior margin of the pterygoid is oblique and the valley between the pterygoid bones is deep and wide, with a width of 90 mm. The vomer is thick, with a thickness of 24 mm, and its lower margin is rounded and separated from the palate. The temporal fossa is just behind M3. The glenoid is slightly convex in lateral view and slightly concave in ventral view. The facet behind the glenoid fossa is wide, smooth, and rough edged. The postglenoid process is short, robust, and converges forward. The basilar tubercle is wide, low, rough, and has a transverse crest behind it. The sagittal crest of the basilar tubercle is weak. The posterior region of the basioccipital is wide, flat, and slightly convex. The basioccipital is at an angle of 165° relative to the basisphenoid.

The posttympanic process is well developed, thick (26.5–31.5 mm), oblique anteroventrally, and fused with the postglenoid process at the lower part of the latter. The external auditory meatus is present and the temporal crest is straight and oblique toward the anterior. The paroccipital process is fused with the posttympanic process and has a tubercular tip. The paroccipital process is vertical; it is conical with three ridges in the male but is slightly more spherical in the female.

The flat palate has a very wide and U-shaped posterior margin level with the middle of M3 and is fused with the vomer. The maxillary tubercle is small and extends posteriorly. The palatal fissure has a long oval shape and extends to the level of the middle of P3.

Mandible—The narrow mandibular symphysis is strongly uplifted, with a sharp alveolar margin and a smooth, concave internal (lingual) surface. The posterior border of the symphysis ends at the level of the middle of p3. The labial surface of the symphyseal region is convex and has two medium-sized nutritive foramina. The symphysis is wider at its anterior than at its posterior end. A slit-like mental foramen is present below p2. The horizontal ramus is very thick, with a thickness of 64 mm at the level of the p4/m1 boundary, a weak sagittal lingual groove, and a curved ventral border. The mandibular angle is rounded and has a projecting edge; the vasal notch is wide and shallow. The ascending ramus is vertical and its anterior margin is 70 mm from m3. The lateral surface of the ascending ramus has a shallow depression in each of its anterior and posterior regions; the an-

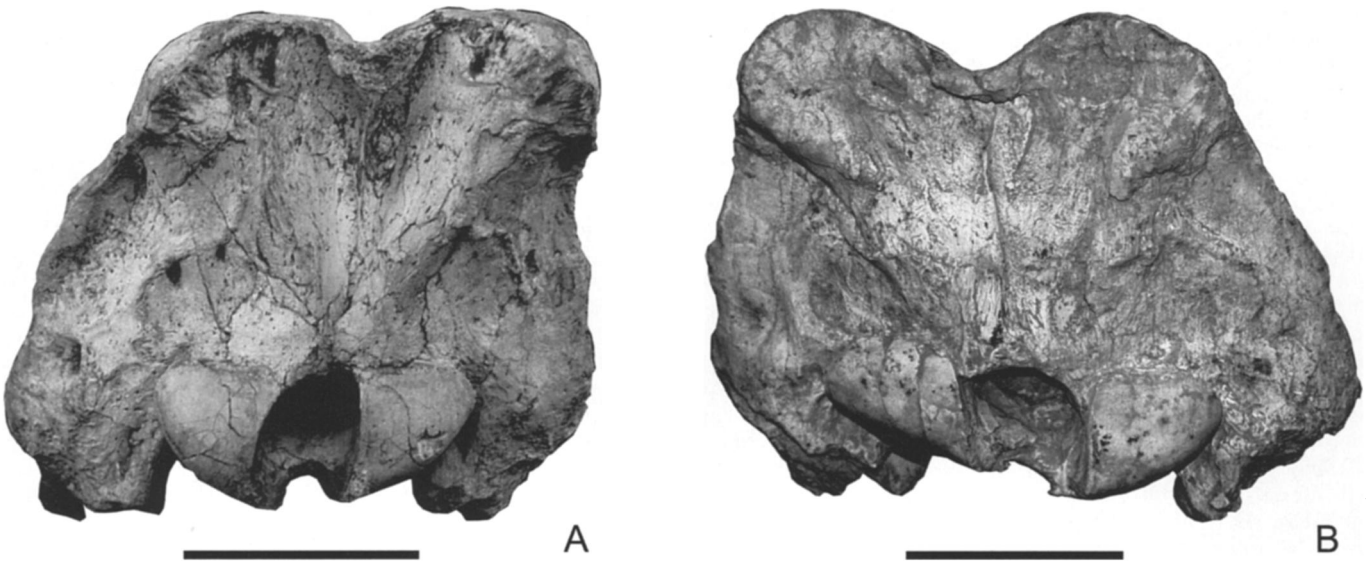

FIGURE 5. Skulls of *Iranotherium morgani*, occipital view. **A**, HMV 1098, female, from Shanzhuang; **B**, HMV 0979, male, from Houshan. Scale bars equal 10 cm.

terior surface is wide and rough in its lower part, but rapidly narrows upward.

Upper Teeth—The cheek teeth are longer in the male than in the female: the length of the premolar row is 141.5 mm in the male but 113.5 mm in the female. HMV 0979 has a freshly erupted M3 and HMV 1098 has a complete molar row that is 172 mm long. The teeth are hypsodont, have wrinkled enamel, and are covered and filled by cement. Because the tooth row of HMV 0979 (Fig. 6B) is slightly worn, its occlusal structures are different from those of HMV 1098 (Fig. 6A): the posterior valley is well developed from P2 to P4 in the former, but is lost or very small in the latter; the median and the posterior valleys are open on M1 and M2 in the former, but are closed in the latter, with the posterior valley being lost on M1. On the upper premolars, the crochet and the antecrochet are absent; the lingual cingulum is weak on P1–2 and absent on P3–4; the metaloph is oblique toward the posterior; the lingual margin of the protocone is rounded; the labial surface is flat with a weak paracone fold; the parastyle is wide and short. DP1 is well developed, with an anterolingual cingulum, and overlaps P2; its hypocone is triangular and isolated and the crista is tiny; its paracone fold slants backward like the mesostyle. P2 has the protocone combined with the hypocone; its protoloph is very narrow and connected with the

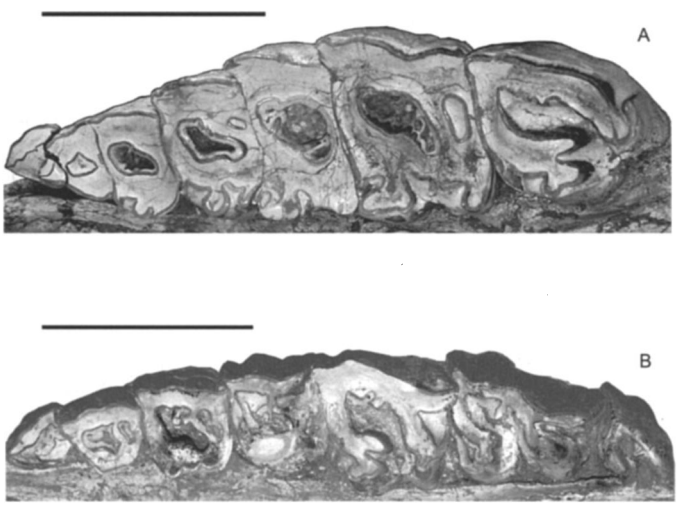

FIGURE 6. Upper teeth of *Iranotherium morgani*, occlusal view. **A**, HMV 1098, female, from Shanzhuang; **B**, HMV 0979, male, from Houshan. Scale bars equal 10 cm.

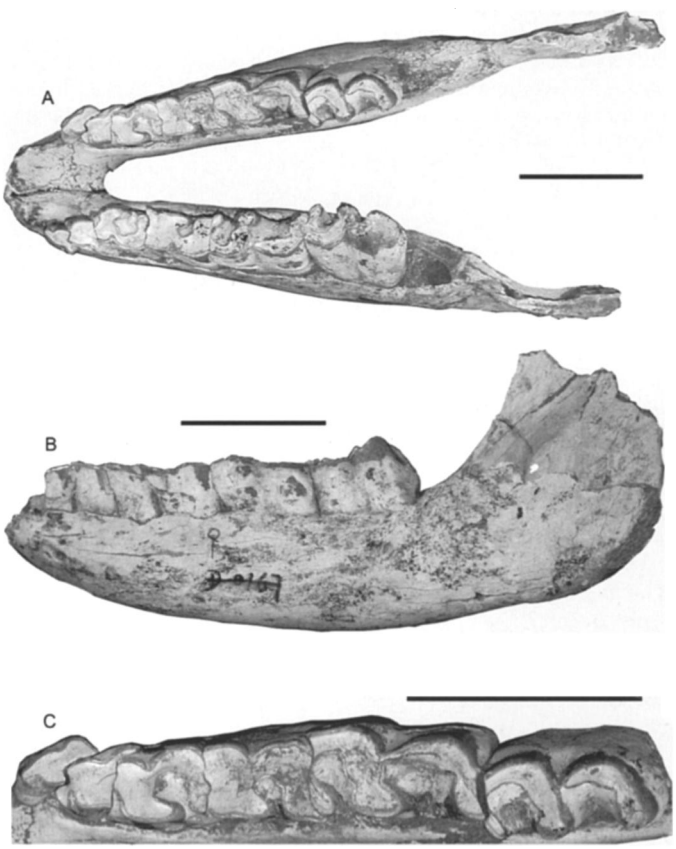

FIGURE 7. Mandible of *Iranotherium morgani*, HMV 1099, from Houshan. **A**, occlusal view; **B**, lateral view; **C**, lower teeth, occlusal view. Scale bars equal 10 cm.

ectoloph; the crista is absent. P3–4 have a narrow lingual valley that is shallow on P3 but deep on P4; the protocone is strongly constricted and the bridge is wide; the crista and postcrista are very weak; the hypocone is not constricted on P3 but is strongly so on P4; the anterior valley is very wide and deep. On the upper molars, the antecrochet is very strong and extends backward; the crochet is absent on M1–2 and weak on M3. The crista is very weak. The lingual cingulum becomes pillar shaped on M1-2 and absent on M3; the lingual margin of the protocone is rounded on M1 but flat on M2-3. The labial surface is convex on M1 and M3 but concave on M2. The parastyle is very short and wide. The anterior cingulum is absent on M1-2 but strong on M3; the anterior groove is closed on M1, narrow and short on M2, and narrow and long on M3. The protocone is strongly constricted; the paracone fold is absent. The metastyle is absent on M1 but long on M2. The metaloph is long. The metacone fold is absent on M1 but deep on M2. The cristella and postcrista are absent on M1 and very weak on M2. The posterior cingulum is absent on M1 but continuous on M2. The hypocone is strongly constricted on M1-2. M1 has two narrow and long antecristae and M2 has five weak ones. The posterior valley is absent on M1. M2 has a weak lingual groove on the base of the protocone. The occlusal surface of M3 is triangular in shape; its protocone has a lingual groove; the protoloph is strongly oblique toward the posterior and the ectometaloph has a posterior groove; the posterior cingulum has a thick, high, and flat surface.

Lower Teeth—The lower premolar row is much shorter than the lower molar row, with the former being 77 mm and the latter 194 mm. The i2 is lost, but its small alveolus is present. On the lower teeth, the labial groove is deeply V-shaped and the trigonid is acute or right-angled; the paralophid is narrow and long; the metaconid is strongly constricted and the entoconid is slightly constricted. On the lower premolars, the lingual entrance of the posterior valley is narrow and the lingual cingulum is absent. The p2 is small, double-rooted, overlaps p3, and has a posterior valley; its paralophid is narrow and the paraconid is reduced. The p3 markedly overlaps p4. On the lower molars, the hypolophid is oblique toward the posterior, and the lingual groove of the entoconid is absent.

COMPARISONS

Pohlig and Keyser (1885) studied the rhinocerotids from Maragha, Iran, including *Rhinoceros* var. *tichorhinus*, which Kittl (1887) referred to as *Aceratherium* aff. *antiquitatis*. Mecquenem (1908) recognized that this species was similar to the rhino *Elasmotherium* and was the ancestor of the latter. When he described it as a new species, however, Mecquenem strangely referred this species to the genus *Rhinoceros*, i.e., as *R. morgani*. Mecquenem (1924) further described the material of *R. morgani* from Maragha. Ringström (1924) suggested that this species did not belong in *Rhinoceros*, referring it to his new genus *Iranotherium* as *I. morgani*.

The studied skulls and mandible from the Linxia Basin, especially HMV 0979 and HMV 1099, are generally similar to the skull and mandible of *Iranotherium morgani* from Maragha, with minor differences.

A marked difference between the specimens from Linxia and Maragha exists in the length ratio of lower premolars to molars. Because the p2 strongly overlaps with p3, which also markedly overlaps with p4, the premolar row on the Linxia mandible is very short, with a ratio of 0.4 to its molar row. On the other hand, the p2 does not overlap with p3 on the Maragha mandible (Mecquenem, 1908:pl. IX, figs. 4, 5), resulting in the ratio of the premolar to the molar rows being 0.6. We think that this difference is due to individual or sexual variations and is not sufficient for establishing a new species.

The skulls of *I. morgani* from Linxia are relatively complete; therefore, additional cranial characters are recognized in this species. Because the Maragha skull lacks the front teeth anterior to P3 (Mecquenem, 1908:pl. VIII, fig. 3, pl. IX, fig. 1), Ringström (1924) guessed that the upper dental formula was 0.0.3.3. On the other hand, we found that DP1 is well developed on both skulls of HMV 0979 and HMV 1098.

HMV 0979 is a young individual, and HMV 1098 is an adult. These two specimens have varying degrees of wear on their teeth, and we can observe the variation on occlusal surfaces (Fig. 6). The labial surface is flatter and the paracone rib is weaker on the lower region. The freshly erupted teeth lack an anterior groove, which is well developed toward the base. On the lightly worn P3-4, the crochet is strong; most notably, the crochet of P4 is bifurcate. In contrast, the crochet is completely absent on all moderately worn premolars. The posterior valley is close to the crown of the premolars and is small or absent toward the base. P2-3 have a close lingual valley, which disappears along with an increase in the degree of wear. The crista of P2, as well as the medifossette and the cristella of P3, disappear in the same manner. The hypocone is constricted on P3 but not on P4 at the slightly worn level, while it is constricted on P4 but not on P3 at the moderately worn level. The crista of the molars is very strong, but becomes very weak toward the base. The parastyle of the molars is narrow and long, but becomes wide and short. The antecrochet on the slightly worn M1-2 is separate from the hypocone. On the upper part of the M1 crown, the posterior valley is present but the antecrista is absent. On that of the M2, the hypocone is not constricted and the antecrista is absent. On the upper part of the M3, the crochet is strong, the protocone is not constricted, and the antecrochet is absent.

SEXUAL DIMORPHISM

Loose (1975) considered that the skulls of two extant rhinoceros species, *Ceratotherium simum* and *Diceros bicornis*, are not dimorphic. Prothero and Sereno (1982) and Prothero (2005) argued that significant size dimorphism is rare in rhinoceroses. They showed that many rhino taxa have horn dimorphism, but others do not, although males tend to have more robust skulls.

On the other hand, Osborn (1898a) concluded that skulls of *Teleoceras* could be identified to gender on the basis of lower tusk diameter and possibly by the size of the terminal horn boss, but he did not provide measurements. Osborn (1898b) found that the gender of the Oligocene rhinocerotids *Subhyracodon occidentalis* and *S. tridactylum* could be determined by their lower-tusk morphology. He also noted the dimorphic character of the nasals-horn bosses that are present in males of the late Oligocene rhinoceros *Diceratherium*. Peterson (1920) pointed out a similarly dimorphic nature of the horn bosses in the early Miocene rhinoceros *Menoceras*. Radinsky (1967) suggested the presence of sexual dimorphism in the primitive rhinocerotoid *Hyrachyus* based on bimodality in molar row lengths. Borsuk-Bialynicka (1973) found that bimodality in the occiput width, maximum skull length, orbit-nuchal crest length, and orbit-nares length supported the conclusion of sexual dimorphism in *Coelodonta antiquitatis*. Voorhies and Stover (1978) confirmed the gender of individuals by their association with fetal remains. Fortelius and Kappelman (1993) referred the bimodality in body mass of *Indricotherium transouralicum* to the perpetual problem of sexual dimorphism in fossil organisms. Mead (2000) and Deng (2001) recognized the sexual dimorphism in *Teleoceras major* and *Chilotherium wimani*, respectively.

The skull of *Iranotherium morgani* from Maragha has a strong hemispherical hypertrophy with a very rough surface on the posterior region of the zygomatic arch (Mecquenem, 1908:pl. VIII, figs. 1, 2). Mecquenem (1908) considered this character to be similar to that of *Sus erymanthius* or hippopotamuses, but Ringström (1924) thought it impossible to explain the function of this

structure. Among the skulls of *I. morgani* from Linxia, HMV 0979 has the hemispherical hypertrophy on its zygomatic arches (Fig. 2B, 3B), but HMV 1098 has no such structure (Fig. 2A, 3A). Moreover, the nasal horn boss of HMV 0979 (Fig. 2B) is much stronger than that of HMV 1098 (Fig. 2A). As a result, we believe that the two skulls from Linxia represent a male and a female of *I. morgani*, respectively, and that the skull from Maragha belongs to a male.

Comparing HMV 0979 and HMV 1098, we find additional sexual dimorphic characters of *I. morgani*. The zygomatic arch of the male is thicker than that of the female. The anterior part of the nasals is wide and rough in the male, but narrow and smooth in the female; this difference is related to the huge horn boss in the male and the smaller horn boss in the female. Because the nasal horn boss of the male is a large dome, its central nasal groove is distinctly deeper than that of the female. The nasal horn boss of the male is much rougher and likely to have supported a larger horn than that of the female. The skull roof of the male is less concave than that of the female, and the frontal region of the male is more convex than that of the female. Therefore, the structure of the whole skull of the male is more robust than that of the female. The braincase of the male is lower, wider, and has more declined outer walls than that of the female, indicating that the male is more massive.

The sexually dimorphic characters of the male and female skulls of *I. morgani* show that the male skull is more massive, with a larger nasal horn and stronger zygomas. These features, especially the huge nasal horn, could be used for defense or competition for mates. Rough prominences on a rhino's skull are generally considered to be horn bosses, as they were associated with the terminal nasal horn (Qiu and Yan, 1982; Ginsburg and Heissig, 1989). The number of horns on a rhinoceros is generally constant, but is occasionally variable. The African black rhinoceros has two horns, but occasionally there is a third horn. Three-horned rhinoceros were found frequently in Northern Rhodesia. There have been reports of a five-horned rhinoceros and of others with horns growing out of their bodies. The great Indian rhinoceros on a famous drawing by Albrecht Durer has a small horn on the shoulder (Grzimek et al., 1972). The hemispherical hypertrophy on the posterior region of the zygomatic arch of the male *I. morgani* could have supported a horn-like callused structure for combat or for display. Because these hypertrophies are different from the horn boss rugosities associated with the true horns in rhinos, they are probably indicative of the presence of larger masseteric and temporal muscles and the overall robustness of the skull.

Iranotherium morgani had hypsodont cheek teeth with wrinkled enamel and rich cement; thus, it apparently was a grazer. The absolute body size of an herbivore is very important in determining the fiber/protein ratio that an animal will be able to tolerate in its diet, as larger animals require proportionately less protein and will be able to tolerate a larger proportion of cellulose (Janis, 1976). Therefore, the giant body size of *I. morgani* implies that this species grazed high-fiber grasses. *I. morgani* obviously inhabited an open grassland.

Significant sexual dimorphism is evident in some rhinocerotid species from cranial characters, such as those in *Teleoceras major* (Mead, 2000). Although HMV 0979 belonged to a young individual, its several cranial measurements differ significantly from those of HMV 1098. The male's (HMV 0979) mean values for maximum breadths of the occiput, the cranial roof, the zygomatic arch, and the palate are distinctly larger than those of the female (HMV 1098).

Cladistic analyses suggest that *Iranotherium* lies within the lineage of the extant rhinoceroses in the subfamily Rhinocerotinae (Cerdeño, 1995) or the lineage of the extinct elasmotheres in the subfamily Elasmotheriinae, which is the sister group of the Rhinocerotinae (Antoine, 2002). Therefore, it is legitimate to compare *Iranotherium* with modern rhinoceroses in the determination of sexual dimorphism.

In extant rhinos, males are commonly more robust than females (Heller, 1913; Laurie, 1982; Hillman-Smith et al., 1986; Owen-Smith, 1988; Rachlow and Berger, 1997; Rachlow et al., 1998). But *Diceros bicornis* does not exhibit obvious sexual dimorphism in body size (Freeman and King, 1969; Hamilton and King, 1969; Owen-Smith, 1988; Hillman-Smith and Groves, 1994; Berger and Cunningham, 1998). The males of the Asian rhinoceroses typically have longer horns with a larger basal girth than do the females. The greater girth is correlated as a rule to the greater width of the horn area of the nasal bones and with its coarser tuberculation or granulation in the male. The horn of the male *Rhinoceros sondaicus* is comparatively well developed, whereas the horn of the female is very small or absent (Pocock, 1946). Males show significantly larger values for basal circumference of the horn, and nasal breadth (Groves, 1982; Dinerstein, 1991). The difference in nasal breadth generally reflects the condition of better-developed horns in males (Pocock, 1946).

Theoretically, the degree of sexual dimorphism in ungulates should reflect the nature of the breeding system (Mead, 2000). On the other hand, Mihlbachler (in press) suggested that sexual dimorphism provides no support for the popular belief that *Teleoceras* was ecologically or behaviorally convergent upon *Hippopotamus* or other large, herding artiodactyls. A significant correlation exists between the degree of sexual dimorphism and harem size in extant ungulates, indicating that most polygynous ungulates live in large groups in open grassland environments (Alexander et al., 1979). Sexual dimorphism in ungulates should be favored in breeding systems where females congregate in small areas (Owen-Smith, 1988). The large, grazing *C. simum* and mixed-feeding *R. unicornis* show a greater degree of sexual dimorphism and have higher female-to-male ratios than do browsing rhinoceros species (Laurie, 1982). The males of *C. simum* defend exclusive territories where a number of females are likely to congregate, and large size in males is beneficial for territory defense (Owen-Smith, 1988). *Rhinoceros unicornis* does not exhibit true territoriality, but the dominant males live in the area of highest adult female concentration (Laurie, 1982). In the browsing *D. bicornis*, horn size correlates with dominance in mature bulls, and male death (excluding poaching) due to intrasexual combat may be as high as 50% (Berger, 1994; Berger and Cunningham, 1998). As with *C. simum* and *R. unicornis*, *D. bicornis* is polygynous (Goddard, 1966).

Webb (1969) interpreted "two healed-over wounds" on the nasals of a male *Teleoceras* cranium from Burge Quarry as evidence of intrasexual aggression. From cranial characters, *Iranotherium morgani* shows more sexual dimorphism than any of the extant rhinoceros species. Judging by its huge nasal horn and the large, robust areas on the dorsal zygomas that supported larger masseteric and temporalis musculature in this species, fights for mating rights may have been violent, perhaps sometimes resulting in death, as do battles between extant hippopotamuses (Eltringham, 1999). What is known of horn function in rhinoceroses? Little, other than that horns are used in combat (Owen-Smith, 1975). One territorial male *C. simum* was observed to be killed in a fight with a neighboring territory holder (Rachlow et al., 1998). The huge nasal horn and the robust skull in males of *I. morgani* could have been used for similar head-on display as in the extant *R. unicornis* (Dinerstein, 1991).

BIOSTRATIGRAPHY AND PALEOECOLOGY

The mammalian fauna of *Iranotherium morgani* from Houshan and Shanzhuang localities is composed of early late Miocene taxa, such as *Dinocrocuta gigantea*. Other well-represented components of the early late Miocene fauna in China include *Hipparion weihoense* and *H. chiai*. These two species of *Hipparion*

have large sizes, deep preorbital fossae far from the orbit, and narrow and long protocones. These characters show that both species apparently belong to the *H. primigenius* group and the hipparionines of this group from Europe and Africa are predominantly Vallesian in age (Qiu et al., 1987). The shared species in the early late Miocene Bahe fauna from Lantian (Shaanxi, China) and the Dashengou fauna include *Tetralophodon exoletus* and *Chleuastochoerus stehlini* (Liu et al., 1978; Zhang et al., 2002). *Hezhengia bohlini* is one of the most typical taxa in the Dashengou fauna. The horncores of *Hezhengia* are less specialized than those of the middle-late late Miocene ovibovines, such as *Plesiaddax*, and its premolars are relatively long with strong ribs and styles. Therefore, the primitive characters of *H. bohlini* imply that its age should be earlier than that of the middle-late late Miocene ovibovines (Qiu et al., 2000). *Acerorhinus hezhengensis* in the Dashengou fauna has a very narrow mandibular symphysis and slightly separated parietal crests that form a high sagittal crest, and thus it is similar to *A. tsaidamensis* in the early late Miocene Qaidam fauna from Qinghai, China, but differs from *A. palaeosinensis* in the late late Miocene Baode fauna from Shanxi, China (Qiu et al., 1988). Judging from all of the components of the Dashengou fauna, it should be correlated to the late Vallesian Age of Europe. Besides the Bahe fauna, the Lamagou fauna from Fugu (Shaanxi, China; Xue et al., 1995) may be contemporaneous with the Dashengou fauna. There are many common taxa between the two faunas, including *Dinocrocuta gigantea*, *Hyaenictitherium wongii*, *Hipparion chiai*, *Chilotherium wimani*, *Samotherium* sp., and *Miotragocerus* sp. Moreover, *Acerorhinus fuguensis* in the Lamagou fauna is very similar to *A. hezhengensis* in the Dshengou fauna (Deng, 2000).

Previously, *Iranotherium morgani* was discovered only from Maragha and Kerjavol in Iran (Antoine, 2002). In Maragha, *I. morgani* belongs to the middle local biozones of the Maragha fauna, accompanying *Hipparion prostylum* (Bernor et al., 1996). Mein (1990) and Steininger et al. (1990) correlated the middle Maragha fauna to the late early and middle Turolian (late MN 11 and early MN 12), between 9.3 Ma and 7.75 Ma. Bernor et al. (1996) suggested that the Maragha faunal sequence correlates with basal MN 11 to middle MN 12, ca. 9 to 7.6 Ma and *I. morgani* may have first appeared in MN 11. Because the fauna that bears *I. morgani* from Linxia can be correlated to the late Vallesian (late MN 9 and MN 10), *I. morgani* appeared in Linxia earlier than in Maragha. The evolutionary center of the tribe Elasmotheriini remains in Asia (Heissig, 1999) and *I. morgani* is likely to have first appeared in northwestern China and then dispersed westward to central Asia.

The late Miocene mammal fossils from Maragha, Samos, and Pikermi were suggested to represent the climax development of the 'savanna faunas' with a great abundance of grazing and cursorial types, which succeeded more forested, warm-temperate biotopes in Western and Central Eurasia and in the Mediterranean Basin during the Late Cenozoic (see Bernor et al., 1996). On the other hand, Solounias et al. (1999) proposed that the paleoecologies of the hipparion faunas in Eurasia were not African-like savannas, but instead, were sclerophyllous evergreen woodlands. The Eastern Mediterranean was comprised of open habitats and there is evidence of strong seasonality in the late Miocene (Fortelius et al., 1996). The cheek teeth of *I. morgani* are hypsodont with wrinkled enamel, indicating that the species was a grazer in open grassland.

Mesopithecus pentelici and *Indarctos maraghanus* are present in the middle Maragha fauna, but primates and ursids are absent in the Dashengou fauna from Linxia. Giraffids and bovids are much richer in the middle Maragha fauna than in the Dashengou fauna. On the other hand, *Pararhizomys hipparionum* is present in the Dashengou fauna, but rodents are absent in the middle Maragha fauna. Hyaenids and mustelids are much richer in the Dashengou fauna than in the middle Maragha fauna (Fig. 8). Therefore, it is indicated that *I. morgani* lived in a more forested environment in Maragha and in a more open habitat in Linxia. In the Linxia Basin, the late Miocene deposits bearing *I. morgani* and other taxa of the *Hipparion* fauna are red clays. Red clay sediments are wind-blown in origin (Ding et al., 1998), and may have been formed under relatively high monsoonal precipitation (Ding et al., 1999). A pollen analysis of the red clay of the Liushu Formation showed that grasses increased significantly and became dominant, especially xilophilous and subxilophilous grasses, along with some broadleaved taxa of temperate and warm temperate zones. The pollens include mainly *Chenopodium*, *Artemisia*, and Granmineae, and accompany Compositae, Ranunculaceae, Cruciferae, Umbelliferae, Polygonaceae, *Betula*, *Quercus*, *Salix*, *Fraxinus*, Cupressaceae, Taxodiaceae, and *Juniperus*, suggesting that the vegetation of the Liushu Formation belonged to an arid steppe (Ma et al., 1998).

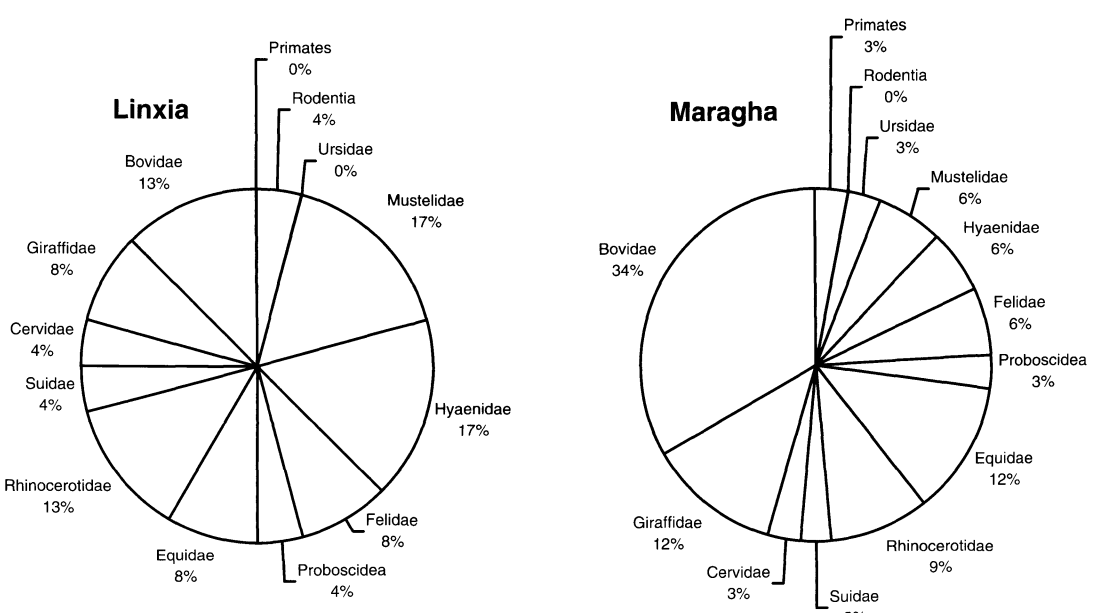

FIGURE 8. Pie charts showing the taxonomic composition of the Linxia and Maragha faunas at the family or the order level.

ACKNOWLEDGMENTS

I thank Prof. Qiu Zhanxiang of IVPP in Beijing, Prof. K. Heissig and Dr. I. Giaourtsakis of BSP in Munich, Dr. Wang Xiaoming of LACM and Prof. D. R. Prothero of Occidental College in Los Angeles, and Dr. M. C. Mihlbachler of AMNH in New York for discussions on the specimens and the manuscript. I am grateful to Prof. Wang Banyue and Dr. Ni Xijun of IVPP for their support in the fieldwork. I thank Dr. D. Biasatti for her improvement of the manuscript in English. This work was supported by the National Science Foundation of China (40232023), the Chinese Academy of Sciences (KZCX2-103, RJZ2001-105), and the Ministry of Science and Technology of China (G2000077700).

LITERATURE CITED

Alexander, R. D., J. L. Hoogland, R. D. Howard, K. M. Noonan, and P. W. Sherman. 1979. Sexual dimorphism and breeding systems in pinnipeds, ungulates, primates, and humans; pp. 402–435 in N. A. Chagnon, and W. Irons (eds.), Evolutionary Biology and Human Social Behavior: an Anthropological Perspective. Duxbury, North Scituate, Massachusetts.

Antoine, P.-O. 2002. Phylogénie et évolution des Elasmtheriina (Mammalia, Rhinocerotidae). Mémoires du Muséum National d'Histoire Naturelle 188:1–359.

Berger, J. 1994. Science, conservation, and black rhinos. Journal of Mammalogy 75:298–308.

Berger, J., and C. Cunningham. 1998. Natural variation in horn size and social dominance and their importance to the conservation of black rhinoceros. Conservation Biology 12:708–711.

Bernor, R. L., N. Solounias, C. C. Swisher, III, and J. A. van Couvering. 1996. The correlation of three classical 'Pikermian' mammal faunas—Maragha, Samos and Pikermi—with the European MN unit system; pp. 137–156 in R. L. Bernor, V. Fahlbusch, and H.–W. Mittmann (eds.), The Evolution of Western Eurasian Neogene Mammal Faunas. Columbia University Press, New York.

Borsuk-Bialynicka, M. 1973. Studies on the Pleistocene rhinoceros *Coelodonta antiquitatis* (Blumenbach). Palaeontologia Polonica 29: 1–95.

Cerdeño, E. 1995. Cladistic analysis of the family Rhinocerotidae (Perissodactyla). American Museum Novitates 3134:1–25.

Deng, T. 2000. A new species of *Acerorhinus* (Perissodactyla, Rhinocerotidae) from the late Miocene in Fugu, Shaanxi, China. Vertebrata PalAsiatica 38:203–217.

Deng, T. 2001. Cranial ontogenesis of *Chilotherium wimani* (Perissodactyla, Rhinocerotidae). Proceedings of the Annual Meeting of the Chinese Society of Vertebrate Paleontology 8:101–112.

Deng, T., X. M. Wang, X. J. Ni, L. P. Liu, and Z. Liang. 2004a. Cenozoic stratigraphic sequence of the Linxia Basin in Gansu, China and its evidence from mammal fossils. Vertebrata PalAsiatica 42:45–66.

Deng, T., X. M. Wang, X. J. Ni, and L. P. Liu. 2004b. Sequence of the Cenozoic mammalian faunas of the Linxia Basin in Gansu, China. Acta Geologica Sinica 78:8–14.

Dinerstein, E. 1991. Sexual dimorphism in the greater one-horned rhinoceros (*Rhinoceros unicornis*). Journal of Mammalogy 72:450–457.

Ding, Z. L., J. M. Sun, T. S. Liu, R. X. Zhu, S. L. Yang, and B. Guo. 1998. Wind-blown origin of the Pliocene red clay formation in the central Loess Plateau, China. Earth and Planetary Science Letters 161: 135–143.

Ding, Z. L., S. F. Xiong, J. M. Sun, S. L. Yang, Z. Y. Gu, and T. S. Liu. 1999. Pedostratigraphy and paleomagnetism of a ~7.0 Ma eolian loess-red clay sequence at Lingtai, Loess Plateau, north-central China and the implications for paleomonsoon evolution. Palaeogeography, Palaeoclimatology, Palaeoecology 152:49–66.

Dollo, L. 1885. Rhinocéros vivants et fossils. Revue des Questions Scientifiques 17:293–300.

Eltringham, S. K. 1999. The Hippos, Natural History and Conservation. Academic Press, London, 256 pp.

Fortelius, M., and J. Kappelman. 1993. The largest land mammal ever imagined. Zoological Journal of the Linnean Society 107:85–101.

Fortelius, M., L. Werdelin, P. Andrews, R. L. Bernor, A. Gentry, L. Humphrey, H.-W. Mittmann, and S. Viranta. 1996. Provinciality, diversity, turnover, and paleoecology in land mammal faunas of the later Miocene of Western Eurasia; pp. 414–448 in R. L. Bernor, V. Fahlbusch, and H.-W. Mittmann (eds.), The Evolution of Western Eurasian Neogene Mammal Faunas. Columbia University Press, New York.

Freeman, G. H., and J. M. King. 1969. Relations amongst various linear measurements and weight for black rhinoceroses in Kenya. East African Wildlife Journal 7:67–72.

Gill, T. 1872. Arrangement of the families of mammals and synoptical tables of characters of the subdivisions of mammals. Smithsonian Miscellaneous Collections 11(1):1–98.

Ginsburg, L., and K. Heissig. 1989. *Hoploaceratherium*, a new generic name for "*Aceratherium*" *tetradactylum*; pp. 418–421 in D. R. Prothero, and R. M. Schoch (eds.), The Evolution of Perissodactyla. Oxford University Press, Oxford.

Goddard, J. 1966. Mating and courtship of the black rhinoceros (*Diceros bicornis* L.). East African Wildlife Journal 4:69–75.

Groves, C. P. 1982. The skulls of Asian rhinoceroses: wild and captive. Zoo Biology 1:251–261.

Grzimek, B., H.-G. Klös, E. M. Lang, and E. Thenius. 1972. Rhinoceros; pp. 34–70 in B. Grzimek (ed.), Grzimek's Animal Life Encyclopedia, Volume 13. Van Nostrand Reinhold Company, New York.

Guérin, C. 1980. Les rhinocéros (Mammalia, Perissodactyla) du Miocène terminal au Pléistocène supérieur en Europe occidentale: comparaison avec les espèces actuelles. Documents du Laboratoire de Géologie de l'Université de Lyon, Sciences de la Terre 79:1–1184.

Hamilton, P. H., and J. M. King. 1969. The fate of black rhinoceroses released in Nairobi National Park. East African Wildlife Journal 7:73–83.

Heissig, K. 1972. Paläontologische und geologische Untersuchungen im Tertiär von Pakistan, 5. Rhinocerotidae (Mamm.) aus den unteren und mittleren Siwalik-Schichten. Bayerische Akademie der Wissenschaften Mathematisch-Naturwissenschaftliche Klasse, Abhandlungen, Neue Folge 152:1–112.

Heissig, K. 1999. Family Rhinocerotidae; pp. 175–188 in G. E. Rössner and K. Heissig (eds.), The Miocene Land Mammals of Europe. Verlag Dr. Friedrich Pfeil, München, Germany.

Heller, E. 1913. The white rhinoceros. Smithsonian Miscellaneous Collections 61:1–77.

Hillman-Smith, A. K. K., and C. P. Groves. 1994. *Diceros bicornis*. Mammalian Species 455:1–8.

Hillman-Smith, A. K. K., R. N. Owen-Smith, J. L. Anderson, A. J. Hall-Martin, and J. P. Selaladi. 1986. Age estimation of the white rhinoceros (*Ceratotherium simum*). Journal of Zoology 210:355–379.

Janis, C. M. 1976. The evolutionary strategy of the Equidae and the origins of rumen and cecal digestion. Evolution 30:757–774.

Kittl, E. 1887. Beiträge zur Kenntniss der fossilen Säugethiere von Maragha in Persien. 1. Carnivoren. Annalen des Naturhistorischen Hofmuseums von Wien 2:317–338.

Laurie, A. 1982. Behavioural ecology of the greater one-horned rhinoceros (*Rhinoceros unicornis*). Journal of Zoology 196:307–341.

Liu, T. S., C. K. Li, and R. J. Zhai. 1978. [Pliocene vertebrates of Lantian, Shensi.] Professional Papers Stratigraphy and Palaeontology 7: 149–200. [Chinese]

Loose, H. 1975. Pleistocene Rhinocerotidae of W. Europe with reference to the Recent two-horned species of Africa and S. E. Asia. Scripta Geologica 33:1–59.

Ma, Y. Z., J. J. Li, and X. M. Fang. 1998. [Records of the climatic variation and pollen flora from the red beds at 30.6–5.0 Ma in Linxia district.] Chinese Science Bulletin 43:301–304. [Chinese]

Matthew, W. D. 1931. Critical observations on the phylogeny of the rhinoceroses. University of California Publications, Bulletin of the Department of Geological Sciences 20(1):1–9.

Mead, A. J. 2000. Sexual dimorphism and paleoecology in *Teleoceras*, a North American Miocene rhinoceros. Paleobiology 26:689–706.

Mecquenem, R., de. 1908. Contribution à l'étude du gisement de vertébras de Maragha et de ses environs. Annales d'Histoire Naturelle, Paris 1(1):27–79.

Mecquenem, R., de. 1924. Contribution à l'étude des fossils de Maragha. Annales de Paléontologie 13:133–160.

Mein, P. 1990. Updating of MN Zones; pp. 73–90 in E. Lindsay, V. Fahlbusch, and P. Mein (eds.), European Neogene Mammal Chronology. Plenum Press, New York.

Mihlbachler, M. C. in press. Sexual dimorphism in Miocene rhinoceroses, *Teleoceras proterum* and *Aphelops malacorhinus*, from Florida. Bulletin of the Florida Museum of Natural History.

Osborn, H. F. 1898a. A complete skeleton of *Teleoceras fossiger*. Notes

upon the growth and sexual characters of this species. Bulletin of the American Museum of Natural History 10:51–59.

Osborn, H. F. 1898b. The extinct rhinoceroses. Memoirs of the American Museum of Natural History 1:75–164.

Owen, R. 1845. A History of British Fossil Mammals and Birds. J. van Voorst, London, 560 pp.

Owen, R. 1848. On the Archetype and Homologies of the Vertebrate Skeleton. J. van Voorst, London, 203 pp.

Owen-Smith, R. N. 1975. The social ethology of the white rhinoceros. Zeitschrift für Tierpsychologie 38:377–384.

Owen-Smith, R. N. 1988. Megaherbivores: the Influence of Very Large Body Size on Ecology. Cambridge University Press, Cambridge, 369 pp.

Peterson, O. A. 1920. The American diceratheres. Memoirs of the Carnegie Museum 7:399–477.

Pocock, R. I. 1946. A sexual difference in the skulls of Asiatic rhinoceroses. Proceedings of the Zoological Society of London 115:319–322.

Pohlig, H., and E. Keyser. 1885. Ueber eine Hipparionen-Fauna von Maragha in Nordpersien, über fossile Elephantenreste Kaukasiens und Persiens und über die Resultate einer Monographie der fossilen Elephanten Deutschlands und Italiens. Zeitschrift Deutschen Geologische Gesellschaft 1885:1022–1027.

Prothero, D. R. 2005. The Evolution of North American Rhinoceroses. Cambridge University Press, Cambridge, U.K., 228 pp.

Prothero, D. R., and P. C. Sereno. 1982. Allometry and paleoecology of medial Miocene dwarf rhinoceroses from the Texas Gulf Coastal Plain. Paleobiology 8:16–30.

Qiu, Z. X., W. L. Huang, and Z. H. Guo. 1987. The Chinese hipparionine fossils. Palaeontologia Sinica, New Series C, 25:1–250. [Chinese 1–193; English 195–250]

Qiu, Z. X., B. Y. Wang, and G. P. Xie. 2000. Preliminary report on a new genus of Ovibovinae from Hezheng district, Gansu, China. Vertebrata PalAsiatica 38:128–134. [Chinese 128–130; English 131–134]

Qiu, Z. X., J. Y. Xie, and D. F. Yan. 1988. A new chilothere skull from Hezheng, Gansu, China, with special reference to the Chinese "*Diceratherium*." Scientia Sinica, Series B 31:494–502.

Qiu, Z. X., and D. F. Yan. 1982. A horned *Chilotherium* skull from Yushe, Shansi. Vertebrata PalAsiatica 20:122–132. [Chinese 122–130; English 130–132]

Rachlow, J. L., and J. Berger. 1997. Conservation implications of patterns of horn regeneration in dehorned white rhinos. Conservation Biology 11:84–91.

Rachlow, J. L., E. V. Berkeley, and J. Berger. 1998. Correlates of male mating strategies in white rhinos (*Ceratotherium simum*). Journal of Mammalogy 79:1317–1324.

Radinsky, L. 1967. *Hyrachyus*, *Chasmotherium*, and the early evolution of helaletid tapiroids. American Museum Novitates 2313:1–23.

Ringström, T. 1924. Nashorner der *Hipparion*-fauna Nord-Chinas. Palaeontologia Sinica, Series C 1(4):1–159.

Solounias, N., J. M. Plavcan, J. Quade, and L. Witmer. 1999. The paleoecology of the Pikermian biome and the savanna myth; pp. 436–453 in J. Agusti, L. Rook, and P. Andrews (eds.), Hominoid Evolution and Climatic Change in Europe, Volume 1: the Evolution of Neogene Terrestrial Ecosystems in Europe. Cambridge University Press, Cambridge.

Steininger, F., R. L. Bernor, and V. Fahlbusch. 1990. European Neogene marine/continental chronologic correlations; pp. 15–46 in E. Lindsay, V. Fahlbusch, and P. Mein (eds.), European Neogene Mammal Chronology. Plenum Press, New York.

Vereshchagin, N. K. 1967. The Mammals of the Caucasus. A History of the Evolution of the Fauna. Israel Program for Scientific Translations, Jerusalem, 609 pp.

Voorhies, M. R., and S. G. Stover. 1978. An articulated fossil skeleton of a pregnant rhinoceros, *Teleoceras major* Hatcher. Proceedings, Nebraska Academy of Sciences 88:47–48.

Webb, S. D. 1969. The Burge and Minnechaduza Clarendonian mammalian faunas of north-central Nebraska. University of California Publications in Geological Sciences 78:1–191.

Xue, X. X., Y. X. Zhang, and L. P. Yue. 1995. Discovery and chronological division of the *Hipparion* fauna in Laogaochuan Village, Fugu County, Shaanxi. Chinese Science Bulletin 40:926–929.

Zhang, Z. Q., A. W. Gentry, A. Kaakinen, L. P. Liu, J. P. Lunkka, Z. D. Qiu, S. Sen, R. S. Scott, L. Werdelin, S. H. Zheng, and M. Fortelius. 2002. Land mammal faunal sequence of the late Miocene of China: new evidence from Lantian, Shaanxi Province. Vertebrata PalAsiatica 40:165–176.

Submitted 1 March 2004; accepted 28 July 2004.